ref 50 can accurately predict the lattice thermal conductivity without any assumption about phonon lifetimes, including the dependence on the phonon mean free path, thus being very useful for phonon engineering by nanostructuring. In the following, we employ this method for evaluating the potential of the transition metal dichalcogenides MX_2 (M = Mo, W; X = S, Se) in thermoelectrics, using WS_2 as an example.

2. METHODOLOGY

Density functional theory based on the Vienna Ab-initio Simulation Package (VASP)[51] is used with plane wave energies up to 500 eV in the expansion of the electronic wave function. The generalized gradient approximation in the Perdew−Burke−Ernzerhof (PBE) flavor is employed for the exchange−correlation functional,[52] and the W $5d^4$ and $6s^2$ electrons, as well as the S $3s^2$ and $3p^4$ electrons, are considered as valence electrons. Moreover, the tetrahedron method with Blöchl corrections is employed.[53] In studying thermoelectric properties, an accurate band structure is of crucial importance because the Seebeck coefficient, electrical conductivity, and electronic contribution to the thermal conductivity depend on it. Within the PBE scheme, we employ a 42 × 42 × 12 *k*-point mesh and afterward shift the conduction states to higher energy to reproduce the experimental band gap. Using a 30 × 30 × 9 *k*-point mesh, an accurate band gap is directly achieved by the HSE06 hybrid functional,[54] which models the short-range exchange energy of the electrons by fractions of Fock exchange and PBE exchange.[55] Because the 2H-WS_2 structure under study has hexagonal symmetry,[56] Γ-centered *k*-meshes of 24 × 24 × 6 *k*-points are used for the Brillouin zone integrations in the structural relaxation. Spin-polarized calculations result in zero magnetic moment, in agreement with the nonmagnetic nature of bulk 2H-WS_2, and therefore can be avoided. 2H-WS_2 consists of slabs of W layers sandwiched between S layers. Bonding within the slabs is covalent, whereas bonding between the slabs is due to van der Waals forces. Standard density functionals do not include the van der Waals interaction, while the semiempirical DFT-D3 method by Grimme[57] adds a van der Waals dispersion contribution, which depends on the geometry and exchange−correlation functional to the total energy. This method is used in the following.

The electronic transport problem is solved by semiclassical Boltzmann transport theory within the constant relaxation time approximation for the electron−electron scattering processes. We use BoltzTraP[58] for evaluating the transport coefficients. This code fits an analytical function to the ab initio electronic band structure by writing it as Fourier expansion,[59,60] maintaining the symmetry of the crystal.[61] Extra expansion coefficients guarantee smooth interpolation between data points.[62] The transport coefficients at temperature T and Fermi level μ are calculated from the obtained analytical expression of the conductivity tensor $\bar{\sigma}_{\alpha\beta}(\varepsilon)$, using the Fermi−Dirac distribution function f_0, as

$$\sigma_{\alpha\beta}(T,\mu) = \frac{1}{\Omega}\int \bar{\sigma}_{\alpha\beta}(\varepsilon)\left[-\frac{\partial f_0(T,\varepsilon,\mu)}{\partial \varepsilon}\right]d\varepsilon \quad (1)$$

$$S_{\alpha\beta}(T,\mu) = \frac{1}{eT\Omega\sigma_{\alpha\beta}(T,\mu)}\int \bar{\sigma}_{\alpha\beta}(\varepsilon)(\varepsilon-\mu)\left[-\frac{\partial f_0(T,\varepsilon,\mu)}{\partial \varepsilon}\right]d\varepsilon \quad (2)$$

$$\kappa^{el}_{\alpha\beta}(T,\mu) = \frac{1}{e^2T\Omega}\int \bar{\sigma}_{\alpha\beta}(\varepsilon)(\varepsilon-\mu)^2\left[-\frac{\partial f_0(T,\varepsilon,\mu)}{\partial \varepsilon}\right]d\varepsilon \quad (3)$$

where Ω is the volume of the unit cell, and e is the charge of an electron. Specifically, we employ a mesh with 8100 *k*-points (455 in the irreducible Brillouin zone) to obtain the ab initio band structure and one with 40500 *k*-points for calculating the Fourier expansion.

Heat conduction in semiconductors and insulators happens through lattice vibrations and is determined mainly by phonon−phonon scattering at high temperatures.[63] The lattice vibrations are modeled assuming wave-like atomic displacements[64] and solving the atomic equation of motion.[65] Moreover, the Hamiltonian is expanded in the atomic displacements from the equilibrium positions, where the expansion coefficients of the potential energy are the force constants of various orders. Truncating the expansion at second order results in a harmonic approximation, for which the solutions of the equation of motion are the normal mode polarization vectors and frequencies. In the harmonic approximation, each normal mode vibrates independently of the others, leading to an infinite lattice thermal conductivity. Therefore, higher order force constants are required. Still, the solutions from the harmonic approximation are valuable inputs for solving the Boltzmann transport equation for phonons.[66]

We use a direct method[67] based on a 3 × 3 × 2 supercell for calculating the harmonic dispersion relation[68] and a 6 × 6 × 2 *k*-point mesh for the Brillouin zone integration while evaluating the total energies and forces. The second-order force constants obtained from this approach describe the short-range interaction. Thus, the dynamical matrices constructed from these force constants do not accurately predict the splitting of the longitudinal and transversal optical phonon branches in polar materials,[69] as it is due to long-range dipole−dipole interactions. A nonanalytical correction has been proposed in ref 70. The additional contribution to the dynamical matrix is a function of the Born effective charges and the high frequency static dielectric tensor,[71] which is calculated using density functional perturbation theory as implemented in VASP.[72,73]

The thermal conductivity is lowered by Umklapp scattering processes (the phonon momentum is changed by a reciprocal lattice vector, whereas the energy is conserved). Three phonon scattering events are dominating at room temperature, while events involving four or more phonons can play a role at elevated temperatures.[74] However, such a complex problem is beyond the scope of state-of-the-art ab initio methods. Therefore, we restrict our considerations to three phonon scattering, using a finite difference scheme to calculate the third order force constants in real space.[75] In this scheme, a supercell is constructed such that there is only negligible interaction between atoms in the center and at the boundary. Four or more phonon scattering events increase the resistance at high temperature so that the thermal conductivity evaluated considering only three phonon scattering events is an upper limit. Accordingly, the figure of merit is a lower limit. In our 3 × 3 × 2 supercell, we consider atoms up to fourth nearest neighbors (one at a time) in displacing them simultaneously with a given atom. The induced forces are calculated using the Hellmann−Feynman theorem[76] as implemented in VASP (6 × 6 × 2 *k*-point mesh), and the third-order force constants are obtained from these forces and displacements following the finite difference method.

The phonon distribution at a specific temperature is given by the Bose−Einstein distribution.[77] A temperature gradient across a material results in a heat flow due to the diffusion of phonons from hot to cold. However, these phonons undergo scattering as they pass through the material, which alters the phonon distribution. Under Umklapp scattering the direction is also changed. Boltzmann's transport equation states that the overall rate of change of the phonon distribution must vanish in steady state.[78] Practically, a linear version[63] of the equation is used, in which the derivative of the phonon distribution with respect to the temperature is replaced with a derivative of the equilibrium Bose−Einstein distribution.[79] In single crystals, the phonons are scattered mainly by other phonons. The scattering cross sections are evaluated from the third-order force constants and polarization vectors[80] and the scattering rates for various events are obtained from these cross sections, phonon distribution functions, and mode frequencies, considering the energy and momentum conservation. Phonon scattering times are obtained from the scattering rates. Because each scattering event involves up to three phonons, the scattering time of one of them depends on the scattering times of the others.[81] Therefore, the scattering times have to be calculated self-consistently. The thermal conductivity is as an integral over the Brillouin zone involving the phonon lifetimes along with the group velocities, frequencies, and the equilibrium distribution function.[82] We use the ShengBTE code for solving the linear Boltzmann transport equation numerically.[50] This is a major improvement as compared to the relaxation time approximation for the evaluation of the lattice thermal conductivity. A 33 × 33 × 8 *k*-point mesh is used in the Brillouin zone integration and Gaussian functions approximate the Dirac delta distributions arising from the energy conservation conditions.

dx.doi.org/10.1021/cm503487n | Chem. Mater. 2014, 26, 6628−6637

Table 1. Structural Parameters

	a (Å)	c (Å)	z	E_g (eV)
PBE	3.166	12.431	0.623	1.0
HSE	3.166	12.431	0.623	1.4
experiment	3.155[83]	12.35[83]	0.622[56]	1.4[86,87]

3. RESULTS AND DISCUSSION

The structural parameters of relaxed WS_2 are presented in Table 1 and show close agreement with the experimental values.[56,83] The electronic band structure calculated using the PBE functional and considering the van der Waals interaction is shown in Figure 1a. We find an indirect band gap of 1.0 eV between the path Λ ($\Gamma \leftrightarrow$ K) and the high symmetry point Γ, as expected from the literature,[44,84,85] while the experimental band gap is 1.4 eV.[86] This underestimation is critical for calculating the electronic contribution to the thermoelectric properties. The experimental band gap can be achieved by the HSE hybrid functional with 17% Fock exchange, which is used in the following (Figure 1b). Electron and hole effective masses calculated at the conduction band minimum and valence band maximum are listed in Table 2.

Table 2. Effective Masses Evaluated from the HSE Electronic Band Structure

	effective mass (m_e)	location	path
electron	0.55	Λ	$\Lambda \rightarrow$ K
	0.61	Λ	$\Lambda \rightarrow \Gamma$
hole	0.61	Γ	$\Gamma \rightarrow$ K
	0.61	Γ	$\Gamma \rightarrow$ L

The *xx* and *zz* tensor components of the Seebeck coefficient as a function of the carrier concentration are shown in Figure 2. Single-crystal WS_2 thermopower measurements in the temperature range of 303−423 K have found a p-type state with a carrier concentration of 1.17×10^{16} cm^{-3}.[88] The experimental Seebeck coefficient of 885 μV/K at 308 K agrees well with our

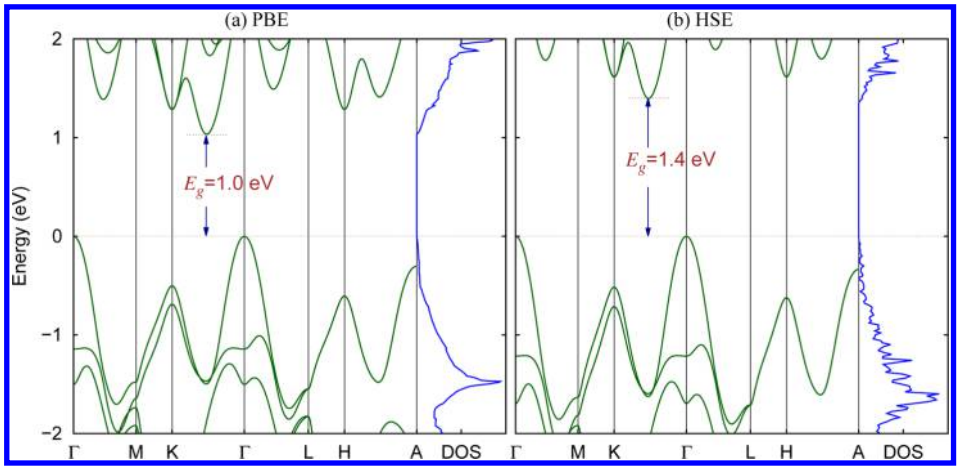

Figure 1. Electronic band structures calculated including the van der Waals interaction: (a) PBE and (b) HSE.

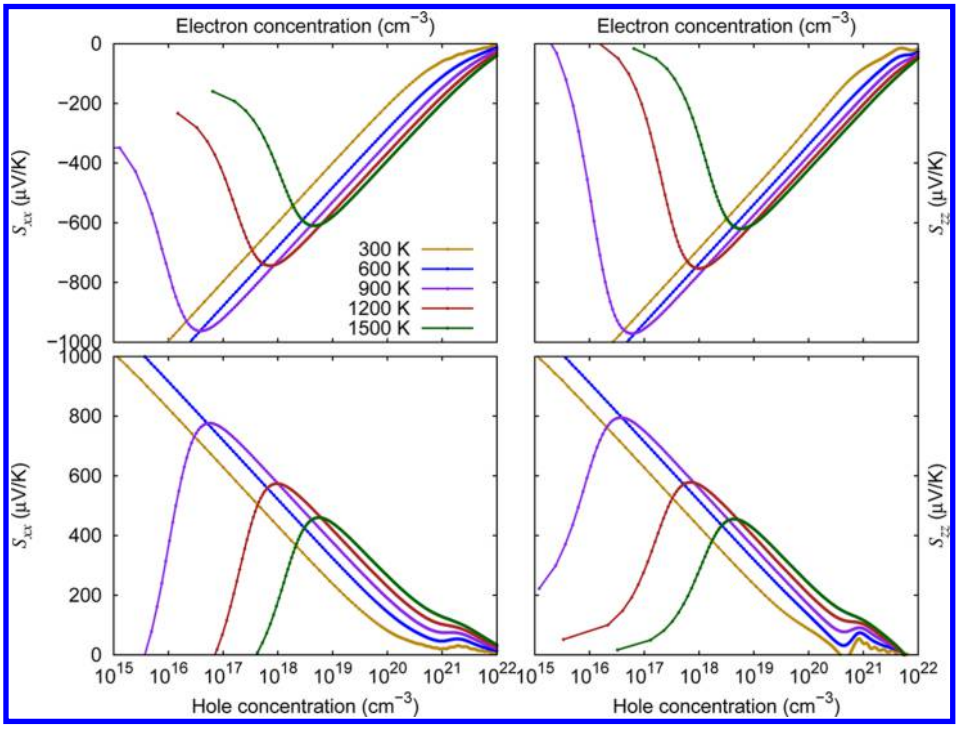

Figure 2. Seebeck coefficient as a function of the carrier concentration.

dx.doi.org/10.1021/cm503487n | *Chem. Mater.* 2014, 26, 6628−6637

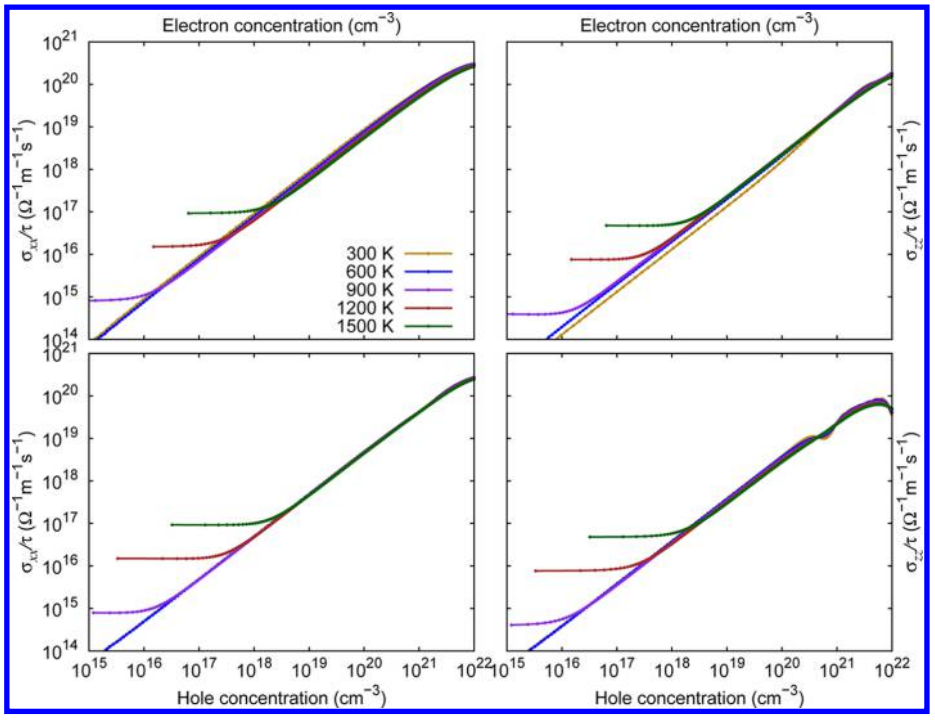

Figure 3. Electrical conductivity as a function of the carrier concentration.

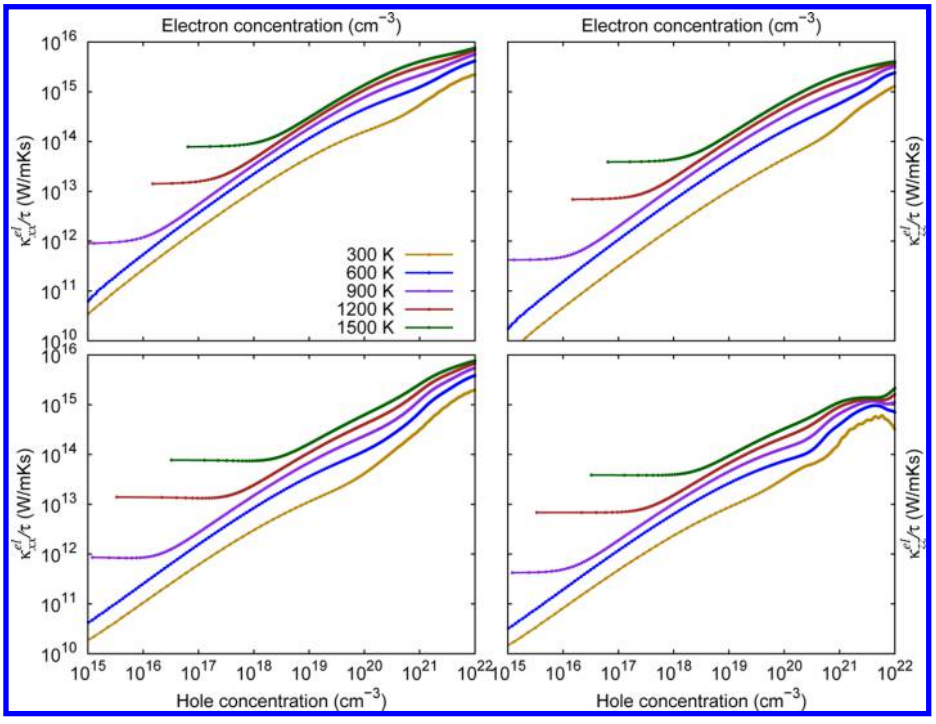

Figure 4. Electronic contribution to the thermal conductivity as a function of the carrier concentration.

calculated value of 815 μV/K for the same hole concentration and temperature. This agreement is due to the accurate representation of the band structure by the HSE functional. The electrical conductivity evaluated from the band structure is addressed in Figure 3, and the electronic contribution to the thermal conductivity is addressed in Figure 4. The electrical conductivity from experiments on a WS_2 polycrystal at 300 K with hole concentration 1.4×10^{17} cm^{-3} was reported to be 240 Ω^{-1}m^{-1}.[89] We use the average value of the diagonal components of σ/τ at the experimental carrier concentration and the experimental conductivity to determine the relaxation time $\tau = 3.72 \times 10^{-14}$ s. This is the only experimental input used in our ab initio approach.

The diagonal components of the high-frequency dielectric tensor are presented in Table 3, together with the calculated Born effective charges. The harmonic phonon dispersion relation obtained from the force constants and Table 3 is shown in Figure 5. There is excellent agreement with the bulk phonon dispersion reported by Molina-Sànchez et al.[90] Results from Raman spectroscopy[91,92] and inelastic neutron scattering[93,94]

dx.doi.org/10.1021/cm503487n | Chem. Mater. 2014, 26, 6628−6637